Proceedings of the 25th National and 3rd International ISHMT-ASTFE Heat and Mass Transfer Conference (IHMTC-2019), December 28-31, 2019, IIT Roorkee, Roorkee, India.

IHMTC2019-PCM-441

Study on the Behaviour of Thermal Stratification in Encapsulated PCM-based Storage System

Rudrodip Majumdar[a], Sandip K. Saha[b,*]

[a] EEP, School of Natural Sciences and Engineering, National Institute of Advanced Studies, IISc campus
[b] Department of Mechanical Engineering, IIT Bombay
* Corresponding author email: sandip.saha@iitb.ac.in

ABSTRACT

Using the thermal stratification phenomena in storing energy in thermal energy storage is a promising technology. In this work, we have studied the effect of the addition of encapsulated PCM to enhance thermal stratification in the storage system. We have developed a numerical model based on simplified energy balance equations considering thermal non- equilibrium between encapsulated phase change material (PCM) and heat transfer fluid (HTF), devoid of complicated momentum and energy equations. The effect of the PCM bed location in the storage system and HTF flow rate on the thermal stratification performance is investigated using stratification number, Richardson number, as well as, charging and storage efficiencies for the charging phase. The HTF flow rate is found to significantly affect the thermal stratification in the storage tank. The Richardson number decreases by 400% if the HTF flow rate is doubled from 2 L/min.

Keywords: Phase change material; Thermal stratification; Storage; Latent heat.

NOMENCLATURE

A= Area (m^2)
c_p=Specific heat (J/kg.K)
d_p = Filler particle diameter (m)
D = Diameter of the thermal storage tank (m)
f_l = Average melt fraction
g = Acceleration due to gravity (m/s^2)
G = Mass flux rate ($kg/m^2.s$)
k = Thermal conductivity (W/m.K)
h_{sf}= Interstitial heat transfer coefficient ($W/m^2.K$)
H = Height of thermal energy storage (m)
H_l = PCM bed height from the top (m)
L_c = Characteristic length (m)
L_{lat} = Latent heat of fusion (J/kg)
$\dot{m}$ = Mass flow rate (kg/s)
N = Number of grid points
Nu = Nusselt number
Pr = Prandtl number
Ra = Rayleigh number
Ri = Richardson number
Str= Stratification number
t = Time (s)
T = Temperature (ºC)
ΔT = Temperature difference (ºC)
U = Velocity (m/s)
U_o = Overall heat transfer coefficient ($W/m^2.K$)
V = Volume (m^3)
x = Distance between two adjacent layers (m)

Greek symbols

α= Thermal diffusivity (m^2/s)
β= Volumetric thermal expansion coefficient (K^{-1})
μ= Viscosity (Pa.s)
ε= Efficiency
ϕ= Porosity
ρ= Density (kg/m^3)
τ = Non-dimensional time

Subscripts

amb=Ambient
avg= Average
bed= PCM bed
c= Collector
ch= Charging
eff= Effective
st= Stored
in= Inlet
ini= Initial
l= Liquid
liq= Liquidus
in= Inlet
ini= Initial
o= Outlet

op= Operational
m= Mean
s= Solid
st= Storage
Sol= Solidus
w = Heat transfer fluid

INTRODUCTION

In the context of efficient, as well as, effective thermal energy storage (TES) pertinent to the low-medium temperature (80-150 °C) solar thermal applications, the addition of encapsulated PCM offers an attractive option in enhancing thermal stratification in the storage system. Mawire et al. [1] experimentally evaluated the thermal stratification parameters of an oil/pebble-bed thermal energy storage system. Ebadi et al. [2] used non-linear differential equations to study the melting process, heat transfer, and energy storage characteristics of a bio-based nano-PCM in a vertical cylindrical thermal energy storage (C-TES). Okello et al. [3] conducted experiments on rock bed TES systems to evaluate the thermal de-stratification process for high-temperature applications. Peng et al. [4] investigated a packed bed PCM-based thermal energy storage using molten salt as HTF for high-temperature applications. Yang and Garimella [5] performed a numerical study on a molten-salt thermocline using commercially available molten salt HITEC as the HTF and quartzite rocks as the filler material. Oro et al. [6] studied packed bed thermal energy storage systems for district cooling and heating networks in the Scandinavian countries. Kumar et al. [7] experimentally evaluated the effect of addition of spherical encapsulated PCM on stratification characteristics in a storage tank. More recently, Majumdar and Saha [8] extensively studied the effect of different geometrical and process parameters on the extent of stratification in the storage tank using a novel numerical method.

Several researchers previously investigated TES tanks filled with various heat transfer fluids (HTF) by employing different filler materials tanks to improve the stratification performance. Although the effect of encapsulated PCM on the thermal performance of TES has been investigated experimentally by few researchers for charging process, the degree of stratification in TES partially filled with encapsulated PCM is found to depend on several external parameters, such as the tank geometry, operating conditions and the choice of the encapsulated material; detailed studies pertinent to such systems are scarcely available in the published literature. Hence, we have studied the effect of PCM bed location and HTF flow rate on the thermal stratification performance using a novel numerical method developed by Majumdar and Saha [8].

DESCRIPTION OF PHYSICAL PROBLEM

Figure 1(a) shows the schematic diagram of a cylindrical storage tank having dimensions of ϕ400 mm (diameter) × 1000 mm (height). A commercial PCM, OM 48 of Pluss India, having a melting temperature of 45-50 °C is considered upon looking at the temperature requirements for domestic hot water (DHW) systems; whereas water is chosen as the HTF. The thermophysical properties of OM 48 are shown in table 1. In this study, the PCM bed height (H_{bed}), encapsulation diameter (d_p) and HTF inlet temperature are kept constant at 400 mm, 75 mm and 60 °C with initial and ambient temperature of 25 °C to study the stratification performance of the storage tank during the charging duration of 120 min (t_{op}).

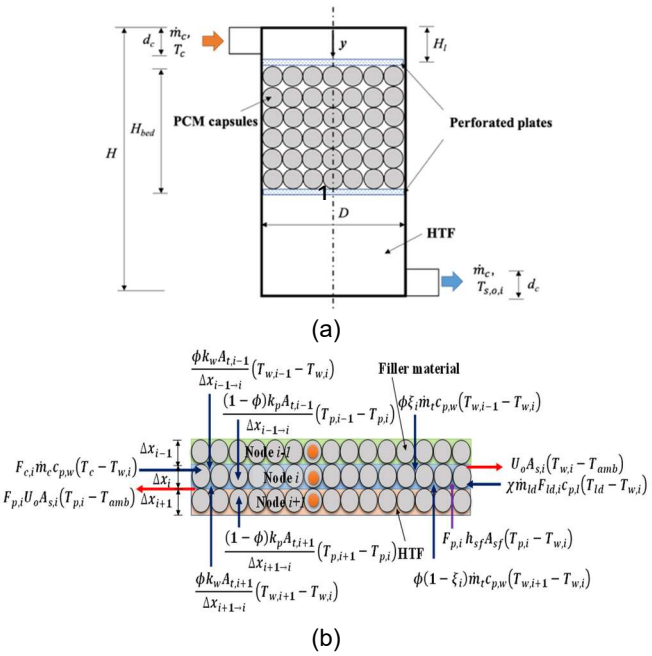

Figure 1: Schematic representation of (a) storage tank and (b) energy flow diagram

Table 1: Thermophysical properties of PCM (OM 48)

Phase	ρ (kg/m^3)	c_p (J/kg.K)	k (W/m.K)	L_{lat} (J/kg)	T_m (°C)
Solid	960	2020	0.2	173500	45
Liquid	875	2350	0.12		50

NUMERICAL MODEL

We have developed a numerical model based on Close model [9] coupled with effective heat capacity method, to assess the thermal stratification behaviour in the storage tank (TES) filled with heat transfer fluid (HTF) and partially filled with encapsulated filler materials. Figure 1(b) shows the energy flow diagram of the control volumes containing HTF and PCM. The change in phase change material (PCM) in the energy balance equation is modelled using effective heat capacity method. The heat transfer fluid and the encapsulated PCMs are in the storage tank is divided into '*N*' layers. In developing a generalized numerical model, we have written individual energy equation for each medium, *viz.* HTF and PCM residing in a layer assuming the absence of thermal equilibrium between HTF and PCM. The energy balance equation considers the addition of energy due to HTF from the collector and the extraction of energy due to HTF flow into the neighbouring layers, as well as, the energy exchange between HTF and PCM. The filler material, encapsulated PCMs, in the storage tank is modelled as the porous media. We have assumed that the flow is laminar, incompressible and well mixed in a layer. We have neglected the volume expansion during melting of PCM in the

capsules and the effect of perforated plates for holding the filler materials on heat transfer. The radiation effect is also neglected. Therefore, two energy equations for the single phase HTF and the solid filler material are written as per figure 1(b), which illustrates the energy flow diagram of a layer (i^{th} node) of porosity ϕ, that contains both heat transfer fluid and the filler material.

Energy equation for HTF:

$$\begin{aligned}\rho_w c_{p,w} V_w \frac{dT_w}{dt} = {} & F_{c,i}\dot{m}_c c_{p,w}\left(T_c - T_{HTF,i}\right) \\ & + \phi\xi_i \dot{m}_t c_{p,w}\left(T_{w,i-1} - T_{w,i}\right) \\ & + \phi(1-\xi_i)\dot{m}_t c_{p,w}\left(T_{w,i+1} - T_{w,i}\right) \\ & + \frac{\phi k_w A_{t,i+1}}{\Delta x_{i+1\to i}}\left(T_{w,i+1} - T_{w,i}\right) \\ & + \frac{\phi k_w A_{t,i-1}}{\Delta x_{i-1\to i}}\left(T_{w,i-1} - T_{w,i}\right) \\ & + U_o A_{s,i}\left(T_{w,i} - T_{amb}\right) \\ & + F_{p,i}\, h_{sf} A_{sf}\left(T_{p,i} - T_{w,i}\right)\end{aligned} \tag{1}$$

Energy equation for PCM filler material:

$$\begin{aligned}\rho_p c_{p,p} V_p \frac{dT_p}{dt} = {} & \frac{(1-\phi)k_p A_{t,i+1}}{\Delta x_{i+1\to i}}\left(T_{p,i+1} - T_{p,i}\right) \\ & + \frac{(1-\phi)k_p A_{t,i-1}}{\Delta x_{i-1\to i}}\left(T_{p,i-1} - T_{p,i}\right) \\ & + F_{p,i} U_o A_{s,i}\left(T_{p,i} - T_{amb}\right) \\ & + F_{p,i}\, h_{sf} A_{sf}\left(T_{w,i} - T_{p,i}\right)\end{aligned} \tag{2}$$

where, $\Delta x_{i-1\to i}$ is the distance between i^{th} and $(i\text{-}1)^{th}$ nodes, $\Delta x_{i+1\to i}$ denotes the distance between i^{th} and $(i+1)^{th}$ nodes. If feed HTF from the collector enters a node, $F_{c,i}$ is set to 1, otherwise it is zero. If the filler material is present in a node, $F_{p,i} = 1$. The term, $\dot{m}_t$ can be calculated as [8],

$$\dot{m}_t = \dot{m}_c \sum_{j=1}^{i-1} F_{c,j} \tag{3}$$

$$\xi_i = \begin{cases} 1 \;\; if\; \dot{m}_t > 0 \\ 0 \;\; if\; \dot{m}_t = 0 \end{cases} \tag{4}$$

The interstitial heat transfer coefficient, $\left(h_{sf}\right)$ in equations (1-2), can be written as [8],

$$Nu_{d_p} = \frac{h_{sf} d_p}{k_w} = 3.6\left(\frac{d_p G}{\mu_w \phi}\right)^{0.365} \tag{5}$$

The superficial area per unit volume of storage tank filled with the filler material, in equations (1-2), is written as, $\frac{A_{sf}}{V} = \frac{6(1-\phi)}{d_p}$.

The overall heat transfer coefficient at the vertical wall of the storage tank can be calculated using the following correlation [8],

$$\overline{Nu}_H = \frac{U_o H}{k_{air}} = 0.68 + \frac{0.670 Ra_H^{\frac{1}{4}}}{\left[1 + \left(\frac{0.492}{Pr}\right)^{\frac{9}{16}}\right]^{\frac{4}{9}}} \; for\; Ra_H \leq 10^9 \; and \; \frac{D}{H} > Ra_H^{-\frac{1}{4}} \tag{6}$$

The overall heat transfer at the top surface can be found from [8],

$$\overline{Nu}_D = \frac{U_o D}{k_{air}} = 0.54 Ra_D^{\frac{1}{4}} \;\; for\; 10^4 \leq Ra_D \leq 10^7, Pr \geq 0.7 \tag{7}$$

and

$$\overline{Nu}_D = \frac{U_o D}{k_{air}} = 0.15 Ra_D^{\frac{1}{3}} \;\; for\; 10^7 \leq Ra_D \leq 10^{11}, all\; Pr \tag{8}$$

The air properties, in equations (6-8), are determined at the film temperature $T_{film} = \frac{T_{surf}(t) + T_{amb}}{2}$ and $Ra_{L_c} = \frac{g\beta L_c^3 (T_{surf}(t) - T_{amb})}{\alpha\gamma}$. We have considered the bottom surface of the storage as insulated.

We have adopted the effective heat capacity method to model phase change in the PCM based filler material [8]. The specific heat of PCM in this model can be written as,

$$c_p = \begin{cases} c_{p,s} & if\; T < T_{sol} \\ c_{p,m} & if\; T_{sol} \leq T \leq T_{liq} \\ c_{p,l} & if\; T > T_{liq} \end{cases} \tag{9}$$

During phase change, the specific heat $\left(c_{p,m}\right)$ is determined from [8],

$$c_{p,m} = (1 - f_l)c_{p,s} + f_l c_{p,l} + \frac{L_{lat}}{T_{liq} - T_{sol}} \tag{10}$$

where,

$$f_l = \frac{T - T_{sol}}{T_{liq} - T_{sol}} \tag{11}$$

We have incorporated the melt convection in liquid PCM by modifying the thermal conductivity of liquid PCM as [8],

$$k_{l,eff} = 0.18 k_l Ra^{0.25} \tag{12}$$

In equation (12), $Ra = \frac{g\beta\left(\frac{d_p}{2}\right)^3 (T(t) - T_{sol})}{\gamma\alpha}$.

We have discretized equations (1-2) using the Finite Difference Method (FDM) and solved implicitly. The transient term is discretized using first order forward difference scheme. We have implemented the formulation in MATLAB. The total number of grids considered in the tank is 71, whereas in the encapsulated PCM bed, it is taken the same as the total number of capsules layers following the grid independence study. The detailed validation of the present model can be found in our previous work [8].

PERFORMANCE PARAMETERS

The non-dimensional time is defined as,

$$\tau = \frac{t}{t_{op}} \tag{13}$$

(a) Stratification number

The stratification number is expressed as [8],

$$Str = \frac{\overline{\left(\frac{\partial T}{\partial x}\right)_t}}{\left(\frac{\partial T}{\partial x}\right)_{max}} \tag{14}$$

where,

$$\overline{\left(\frac{\partial T}{\partial x}\right)_t} = \frac{1}{N-1}\left[\sum_{i=1}^{N-1} \frac{T_i - T_{i+1}}{\Delta x_{i+1\to i}}\right] \tag{15}$$

and

$$\overline{\left(\frac{\partial T}{\partial x}\right)_{max}} = \frac{T_{in} - T_{ini}}{(N-1)\Delta x_{i+1\to i}} \tag{16}$$

(b) Richardson number

Richardson number (Ri) is expressed as [8],

$$Ri = \frac{g\beta H(T_{i=1} - T_{i=N})}{U^2} \tag{17}$$

where,

$$U = \frac{4\dot{m}_c}{\pi d_c^2 \rho_w} \tag{18}$$

where, d_c = collector pipe diameter.

(c) Storage efficiency

The storage efficiency (ε_{st}) is written as [8],

$$\varepsilon_{st} = \frac{T_{avg}(t) - T_{ini}}{T_{in} - T_{ini}} \tag{19}$$

(d) Charging efficiency

The charging efficiency can be estimated using equation (20) as [8,10],

$$\varepsilon_{ch} = \frac{T_{in} - T_o(t)}{T_{in} - T_{ini}} \tag{20}$$

RESULTS AND DISCUSSIONS

Effect of PCM bed location:

The effect of PCM bed location on the stratification performance of the latent heat thermal energy storage tank is investigated by considering three PCM bed locations of 100, 300 and 500 mm from the top of the tank for the flow rate of 2 L/min at the HTF inlet temperature of 60 ºC during the charging operation. The PCM bed height is 400 mm, and the encapsulation PCM diameter is chosen as 75 mm. The porosity of the PCM bed is kept fixed at 0.4085. In the context of characterisation of stratification in the tank, the temporal variation of HTF temperature at the outlet of the tank is of prime interest. At an instant of time, the temperature difference between the top and bottom sections of the tank reflects the extent of thermal stratification in the tank. Figure 2(a) shows the transient variation of HTF outlet temperature for three different PCM bed locations (H_l). It can be observed from the figure that the HTF outlet temperature remains almost same for all the PCM bed locations, however, in case of H_l = 100 mm, the HTF outlet temperature is found to rise at a slightly later instant followed by a rapid increase. The delay in rise in the HTF outlet temperature can be attributed to the presence of encapsulated PCMs at the inlet which melts early, as can be seen from figure 2(b). The initiation of melting of PCM at the earlier stage retards the rate of heat diffusion to the bottom portion of the tank due to absorption of heat in the form of sensible heat and latent heat in the PCM. However, the PCM capsules located near to the inlet of the tank melts faster and reaches ~0.78 at the end of the charging process. As a result, the HTF outlet temperature reaches the inlet temperature slightly earlier than that for other PCM bed locations.

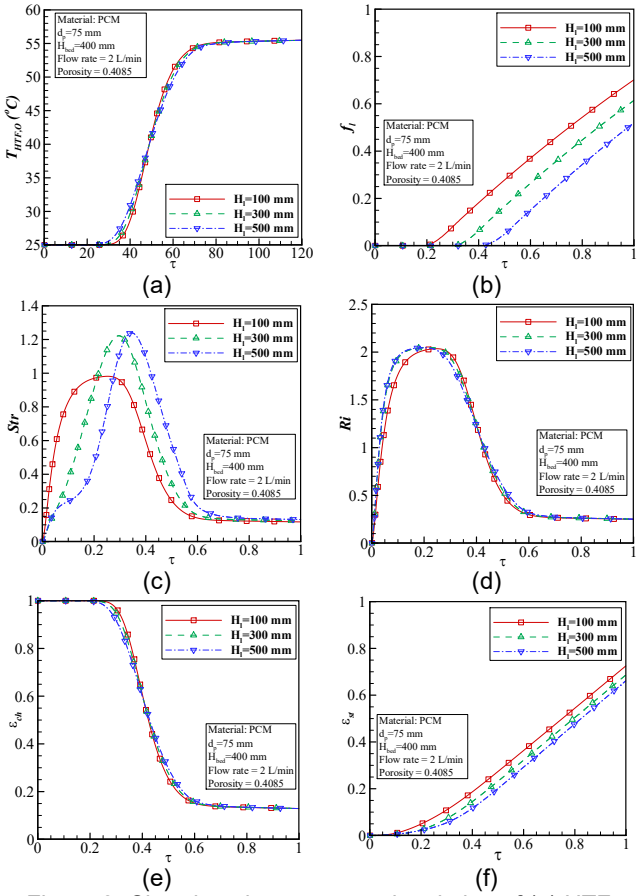

Figure 2: Charging phase temporal variation of (a) HTF temperature at TES tank outlet, (b) average melt fraction of PCM, (c) Stratification number, (d) Richardson number, (e) charging efficiency, and (f) storage efficiency for different PCM bed locations

Figure 2(c) depicts the evolution of the stratification number (Str) for the aforesaid values of the PCM bed locations. The peak value in the stratification number denotes the instant at which the HTF temperature at the outlet of TES tank starts to rise from the initial value [7]. The stratification number is observed to increase monotonically from the starting of the charging process and eventually reaches the maximum value of 0.982, 1.222 and 1.24 for PCM bed location of 100, 300 and 500 mm. The peak value in the stratification number increases with the increase in PCM bed location due to less melting of PCM, resulting in a higher thermal gradient along the tank height. It can be noted that for a particular HTF flow rate and a particular HTF temperature at the tank inlet, the peak value of the stratification number is affected by the depth of temperature penetration from the top of the tank, which depends on the rate of heat diffusion influenced by the PCM bed location. The stratification number decreases sharply after reaching the peak value, signifying a degradation in the thermal stratification; which is due to the reduced thermal gradient in the tank. The decrease in the stratification number

profile is observed to be slower in case of the PCM bed located near the inlet of the tank (H_l = 100 mm). Once the PCM, located at the top section of the tank, starts melting after reaching its melting point, it absorbs heat as the latent heat, resulting in a slower degradation in thermal stratification as a stable thermal gradient is maintained. The *Str* is found to be 0.12, 0.126 and 0.13 for the PCM bed locations of 100, 300 and 500 mm, respectively.

Figure 2(d) shows the transient variation in Richardson number for aforementioned PCM bed locations (*i.e.* H_l = 100, 300 and 500 mm). Higher value of *Ri* indicates better stratification performance. During the beginning of the charging operation, the temperature in the top section of the storage tank increases due to the sensible heating of the solid PCM and water. This results in a sharp rise in the Richardson number, as seen in figure 2(d). The peak value of the Richardson number is observed to remain same (~2.053) for all the PCM bed locations, however the peak value of *Ri* occurs earlier (τ = 0.178) in case of H_l = 500 mm compared to that for the other two cases due to the initiation of melting of PCM at a later instant. Following the peak value, *Ri* sharply decreases as the heat diffusion towards the bottom of the tank increases. However, the rate of decrease in the *Ri* profile is slightly slower for the PCM bed located away from the inlet, as it curbs the amount of heat being diffused towards the tank outlet owing to storage of heat content as the latent heat sitting at the lower-bottom part of the tank and hence the mixing in the HTF occurs in a more gradual manner. The *Ri* value at the end of the charging process is obtained as ~0.25 for all the PCM bed locations.

Figure 2(e) illustrates the variation of charging efficiency for the TES system for multiple PCM bed locations. From the figure, it is observed that the charging efficiency remains fixed at 1, for initial ~25% time of the charging process for all the PCM bed locations of 100, 300 and 500 mm, respectively. The charging efficiency remains slightly higher for a longer initial period of the charging process for the PCM bed located near the inlet, due to the early melting of PCM. Afterwards, a rapid decrease in the charging efficiency is observed over the next ~40% of the time. The charging efficiency reduces as more heat is diffused towards the bottom section of the storage tank. Following the rapid decrease, the charging efficiency remains fixed at a significantly low value of 0.13 for PCM bed locations of 100, 300 and 500 mm at the end of the charging phase.

Figure 2(f) displays the evolution of storage efficiency for different bed locations. By definition, the storage efficiency, at any instant t, stands for the ratio of cumulative heat transferred to the storage tank up to that instant, to the maximum storage capacity of the TES tank. It can be observed from the figure that the storage efficiency increases from its initial value at initial ~1% of the charging period for all the PCM bed locations. It is found that the storage efficiency is 72.1%, 68.6% and 66.1% for PCM bed locations of 100, 300 and 500 mm, respectively at the end of the charging operation. Therefore, it is significantly affected due to the variation of the PCM bed location; as the early melting of PCM for H_l =100 mm leads to storage of more heat in the form of latent heat.

Effect of HTF flow rate:

The HTF flow rate plays an important role on the stratification characteristics of the storage tank, as the energy stored in the storage tank is directly proportional to the HTF flow rate. Figure 3(a) shows the profile of HTF outlet temperature for three different HTF flow rates, *viz.* 2, 3 and 4 L/min for d_p = 75 mm. The PCM bed height is kept fixed at 400 mm and the PCM bed location is maintained at 100 m from the top of the tank. The HTF inlet temperature and the initial and ambient temperatures are maintained at 60 and 25 ºC, respectively. For flow rates of 2, 3 and 4 L/min, the HTF outlet temperature is observed to remain almost at the initial temperature for an initial period of t = 26.8, 19.8 and 14.5 min, respectively. The HTF outlet temperature starts affecting once heat diffused from the top portion to the bottom section of the tank. The $T_{HTF,o}$ sharply increases until 83.2, 51.3 and 36 min for flow rates of 2, 3 and 4 L/min. During the melting of PCM, $T_{HTF,o}$ slowly increases as can be seen in figure 3(b). For higher HTF flow rate, the PCM in capsules melts faster compared to lower HTF flow rate. The HTF outlet temperature finally reaches 55.5, 56.7 and 57.4 °C at the end of the charging phase. Hence, the HTF flow rate significantly affects the energy storage as a higher HTF flow rate stores more heat, resulting in the early reaching of $T_{HTF,o}$ to the inlet temperature level.

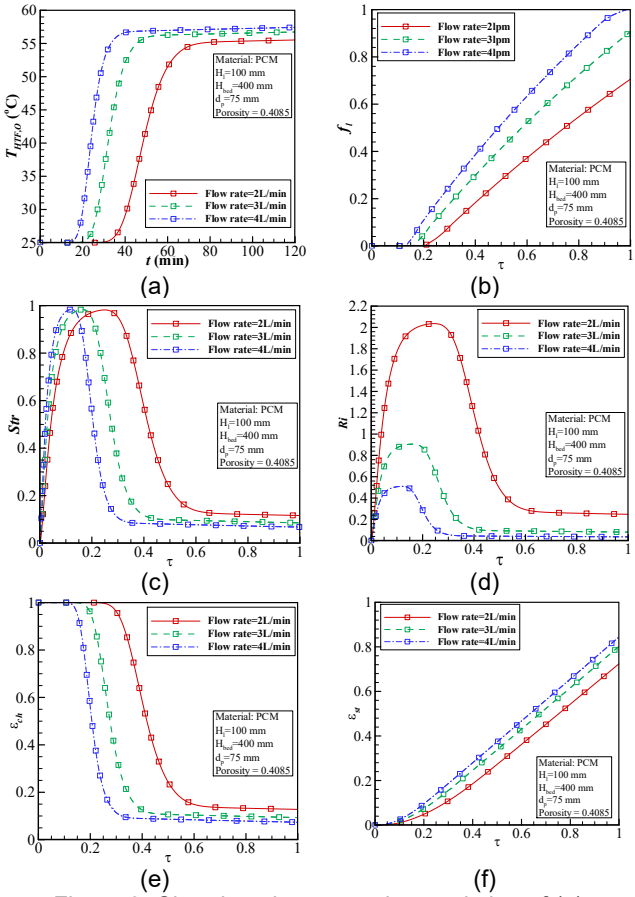

Figure 3: Charging phase transient variation of (a) temperature at TES tank outlet, (b) average melt fraction, (c) stratification number, (d) Richardson number, (e) charging efficiency, and (e) storage efficiency for different flow rates

Figure 3(c) illustrates the transient variation of stratification number for different HTF flow rates. During the charging process, as soon as the hot HTF starts flowing into the TES tank initially at 25 ºC to store energy, the thermal gradient starts to develop across the height of the tank, thereby augmenting the thermal stratification in the tank. The peak value in the stratification number remains almost the same; however, the peak value occurs late for the lower HTF flow rate. This indicates that the lower HTF flow rate affects the HTF outlet temperature at a later time. It can be observed from the figure that the degradation in the stratification is rapid for higher HTF flow rate. Higher stratification is maintained at the end of the charging process by lower HTF flow rate.

Figure 3(d) depicts the evolution of Richardson number for different HTF flow rates. The *Ri* is found to be maximum at 2.04 for HTF flow rate of 2 L/min. The Richardson number decreases with increasing HTF flow rate as evident from equations (16-17). As the HTF flow rate increases, the supplied heat is quickly diffused to the bottom portion of the tank, thereby decreasing the temperature gradient between the top and bottom portions of the tank. The *Ri* value approaches zero, once the temperature gradient in the tank decreases near the end of the charging phase for HTF flow rate of 3 and 4 L/min.

Figure 3(e-f) shows the temporal variation of charging and storage efficiencies for different HTF flow rates. It is evidently observed in figure 3(e) that the charging efficiency remains close to 1 for a longer period for a lower HTF flow rate. This indicates that the energy storage for lower HTF flow rate is more gradual compared to higher HTF flow rate. The same observation can be made in case of storage efficiency (figure 3(f)). The storage efficiency is higher for higher HTF flow rate. If the HTF flow rate is doubled, the storage efficiency is increased by ~16.6% at the end of the charging operation.

Conclusions

In this study, we have evaluated the thermal stratification behaviour in thermal energy storage (TES) partially filled with phase change material (PCM) capsules for charging phase using simplified energy balance equations considering thermal non- equilibrium between encapsulated phase change material (PCM) and heat transfer fluid (HTF). Based on the numerical simulations performed considering different PCM bed locations, as well as, varying HTF flow rates, the following findings are concluded:

- During the charging period, PCM bed location in the TES tank insignificantly affects the thermal stratification behaviour. The occurrence of peak value of stratification number is earlier for the PCM bed located near the inlet, whereas, the peak value of *Ri* occurs earlier for a deeper bed location inside the storage tank.
- The HTF flow rate is the most important parameter governing the thermal stratification in the TES. The peak value of the Richardson number is decreased by 400% if the flow rate is increased from 2 to 4 L/min. The storage efficiency is found to be higher for higher HTF flow rate.

The present findings can be used to analyse and design the thermal energy storage partially filled with PCM capsules, using the thermal stratification phenomena, as per the requirements of the load loop.

References

1. Mawire, A., and S.H. Taole. 2011. “A comparison of experimental thermal stratification parameters for an oil/pebble-bed thermal energy storage (TES) system during charging.” *Applied Energy* 88; 4766–4778.
2. Ebadi, S., S.H. Tasnim, A.A. Aliabadi, and S. Mahmud. 2018. “Melting of nano-PCM inside a cylindrical thermal energy storage system: Numerical study with experimental verification.” *Energy Conversion and Management*, 166: 241-259.
3. Okello, D., O.J. Nydal, and E.J.K. Banda. 2014. “Experimental investigation of thermal de-stratification in rock bed TES systems for high temperature applications.” *Energy Conversion and Management* 86: 125-131.
4. Peng, H., H. Dong, and X. Ling. 2014. “Thermal investigation of PCM-based high temperature thermal energy storage in packed bed.” *Energy Conversion and Management* 81: 420-427.
5. Yang, Z., and S.V. Garimella. 2010. “Thermal analysis of solar thermal energy storage in a molten-salt thermocline.” Solar Energy 84: 974-985.
6. Oró, E., A. Castell, J. Chiu, V. Martin, and L. F. Cabeza. 2013. “Stratification analysis in packed bed thermal energy storage systems.” *Applied Energy* 109: 476–487.
7. Kumar, G.S., D. Nagarajan, L.A. Chidambaram, V. Kumaresan, Y. Ding, and R. Velraj. 2016. “Role of PCM addition on stratification behaviour in a thermal storage tank - An experimental study.” *Energy*, 115: 1168-1178.
8. Majumdar, R., and S.K. Saha. 2019. “Effect of Varying Extent of PCM Capsule Filling on Thermal Stratification Performance of a Storage Tank.” Energy 178: 1-20.
9. Close, D.J.A. 1967. “Design approach for solar processes.” *Solar Energy* 11(2): 112–22.
10. Chan, A.M.C., P.S. Smereka, and D. Giusti. 1983. “A numerical study of transient mixed convection flows in a thermal storage tank.” *Journal of Solar Energy Engineering* 105: 246-253.